29Si NMR shielding tensors in triphenylsilanes – 29Si solid state NMR experiments and DFT-IGLO calculations

ARTICLE *in* ZEITSCHRIFT FÜR ANORGANISCHE UND ALLGEMEINE CHEMIE · MAY 2012

Impact Factor: 1.16 · DOI: 10.1002/zaac.201200107

5 AUTHORS, INCLUDING:

Thomas Heine
Jacobs University
281 PUBLICATIONS **6,117** CITATIONS
SEE PROFILE

Raiker Witter
Tallinn University of Technology
42 PUBLICATIONS **477** CITATIONS
SEE PROFILE

DOI: 10.1002/zaac.201200107

^{29}Si NMR Shielding Tensors in Triphenylsilanes – ^{29}Si Solid State NMR Experiments and DFT-IGLO Calculations

Erica Brendler,*[a] Thomas Heine,[b] Wilhelm Seichter,[c] Jörg Wagler,[d] and Raiker Witter[e]

Dedicated to Professor Berthold Thomas on the Occasion of His 70th Birthday.

Keywords: Triphenylsilanes; ^{29}Si NMR spectroscopy; Chemical shift tensors; Quantum chemical calculation; Crystal structures

Abstract. ^{29}Si NMR shielding tensors of a series of triphenylsilanes Ph_3SiR with R = Ph, Me, F, Cl, Br, OH, OMe, SH, NH_2, $SiPh_3$, C≡CPh were determined from ^{29}Si CP/MAS spectra recorded at low spinning rates. In addition the principal components of the shielding tensor were calculated employing the DFT-IGLO method. For most silanes experimental and calculated values are in good accordance. Larger differences were observed for systems with hydrogen bridge forming substituents and the halides bromide and chloride. In some of the spectra the shielding information interfered with residual dipolar couplings. The different contributions of the various substituents to the principal components of the shielding tensor and the orientation of the tensor within the molecules are discussed and compared for the compounds under investigation.

Introduction

The interpretation of ^{29}Si NMR spectra, e.g. the chemical shifts observed therein, is not as straightforward as in case of ^{1}H or ^{13}C NMR spectra. The variable influence of the diamagnetic and paramagnetic contributions to the chemical shift is expressed in the so called "sagging pattern" of the chemical shift dependence with changing substituents $R_{4-x}R'_xSi$.[1] Thus, the determination of chemical shift data of related compounds and the setting up of ^{29}Si NMR spectroscopic data bases[2,3] proved even more important and valuable than for the nuclei mentioned above.

In addition to the empirical gathering and storing of data, approaches to a particular understanding of the subtle contributions of various substituents appear essential. Thus, in order to get deeper insight into the origin of the chemical shift contributions of the silicon environment, the determination of the ^{29}Si shielding tensor by Solid State NMR spectroscopic measurements together with the quantum chemical calculation of the tensor allows for the interpretation of the contributions of different bonding partners, for the finding of correlations between the chemical shift and molecular structure and environment.[4] Often the principal components of the shielding tensor are more sensitive to electronic changes in the proximity of a nucleus than the isotropic chemical shift. Studies on five- and six-coordinate silicon compounds could benefit from either the large anisotropy of the shielding tensor or the obviously "easy to interpret" directionality with reference to the bonding directions.[5a–i]

Our current study addressed a series of four-coordinate silicon compounds, despite of the fact that the ^{29}Si chemical shift anisotropy of fourfold coordinated silicon compounds is in general comparatively small and it might turn out difficult to interpret the perpendicular shielding tensor components within a tetrahedral system of more or less similar bonding situations. In the presented study a series of triphenylsilanes was chosen, giving the possibility to modify the fourth substituent at silicon by a large variety of groups, always resulting in solids suitable for CP/MAS NMR spectroscopic studies. Early experiments of shielding tensor measurements were carried out by *Gibby* et al.[6] on phenyl and methyl-substituted silanes and by *West* et al.[7a–d] on cyclic and linear silanes as well as disilynes. Recent reports are dealing with Si=*X* multiple bonding.[8] On triphenylsilanes, to the best of our knowledge, the first shielding tensor measurements were done by *Harris* et al.[9] and interpreted with respect to the crystal structure of the compounds, and by *Mäler* et al. combined with relaxation time analysis.[10] During the last years triphenylsilanol was the subject of chemi-

* Dr. E. Brendler
Fax: +49-3731-39-3666
E-Mail: erica.brendler@chemie.tu-freiberg.de
[a] Institut für Analytische Chemie
TU Bergakademie Freiberg
Leipziger Str. 29
09599 Freiberg, Germany
[b] School of Engineering and Science
Theoretical Physics – Theoretical Materials Science
Jacobs-Universität Bremen
P.O. Box 750 561
28725 Bremen, Germany
[c] TU Bergakademie Freiberg
Institut für Organische Chemie
[d] TU Bergakademie Freiberg
Institut für Anorganische Chemie
[e] Institut für Nanotechnologie, KIT
Hermann-von-Helmholtz-Platz 1
76344 Eggenstein-Leopoldshafen, Germany

cal shift studies as a model compound for siloxane systems.[11a–e]

Computational analysis of the molecular systems (i.e., coordinates obtained from X-ray diffraction experiments) by the DFT-IGLO method provides a tool for systematically breaking down the contributions of each substituent to the shielding tensor into a set of Independent Localized Orbitals. It thus provides a helpful basis for discussion of experimentally obtained data – as long as experimental and computational results are well in accord.

Results and Discussion

NMR Measurements

Subject of this study were the triphenylsilanes Ph_3SiR with R = H, CH_3, Ph, NH_2, OH, OCH_3, SH, C≡CPh, F, Cl, Br, $Si(CH_3)_3$, $SiPh_3$. The proton decoupled spinning side band (SSB) ^{29}Si CP/MAS NMR spectra of most of these silanes were dominated by the chemical shift anisotropy. For $R = NH_2$, Cl and Br residual dipolar couplings between silicon and the quadrupolar nucleus resulted in an additional splitting. These contributions were analyzed using the WSOLIDS NMR simulation package.[12] Table 1 lists the parameters used in the simulation of the coupling patterns, Figure 1 and Figure 2 show the experimental spectra together with spectra calculated on basis of the these parameters. Additional experimental effort proved essential for Ph_3SiBr, the residual dipolar couplings of which were at 7 T in the order of magnitude of the span Ω at silicon, which made it impossible to extract the shielding tensor. To reduce the coupling to the quadrupolar nucleus and to verify the simulation additional measurements at 9.4 and 17.6 T were carried out. Ph_3SiBr spectra were simulated separately for both isotopes and proved to be similar. Therefore only the spectra of the isotope ^{79}Br are shown here. Although the measurements at higher field reduced the dipolar interactions, extremely long T_1 values for both silicon and hydrogen together with a poor CP-efficiency (which was observed for all compounds with only phenyl as the hydrogen containing substituent) prevented the measurement of SSB spectra and the extraction of the shielding tensor therefrom.

Table 1. Parameters used for the simulation of the ^{29}Si NMR spectra of Ph_3SiBr, Ph_3SiCl, Ph_3SiNH_2.

Compound	δ_{iso} /ppm	J /Hz	D /Hz	χ /MHz	β /°
Ph_3SiBr	3.5	165	–530.7	–260	13
Ph_3SiCl	3.35	30	–261	31	0
Ph_3SiNH_2	–16.75	12.5	–345	–0.95	0

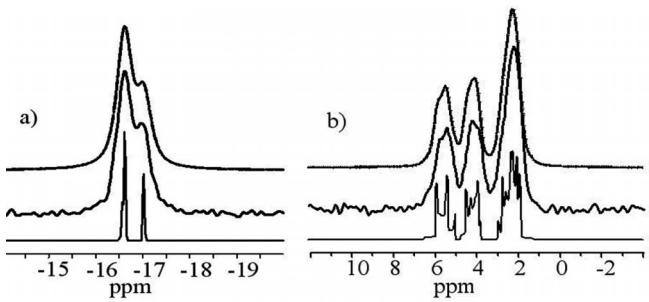

Figure 1. Experimental (middle) and simulated (top with line broadening, lower without) ^{29}Si CP/MAS spectra of a) Ph_3SiNH_2 and b) Ph_3SiCl.

For Ph_3SiNH_2 the $^1J(^{29}Si–^{15}N)$ coupling constant was determined by ^{15}N INEPT measurements in $CDCl_3$ to be 17.6 Hz. The quadrupolar coupling constants were estimated on the basis of NQR measurements on these or related compounds.[13,14] The direct dipolar coupling constants were calculated from the interatomic distances in the crystal structure. Ph_3SiCl and Ph_3SiBr contain two independent molecules in the crystallographic asymmetric unit each, their Si–R distances differ only by 0.003 Å, which is within the limits of experimental error

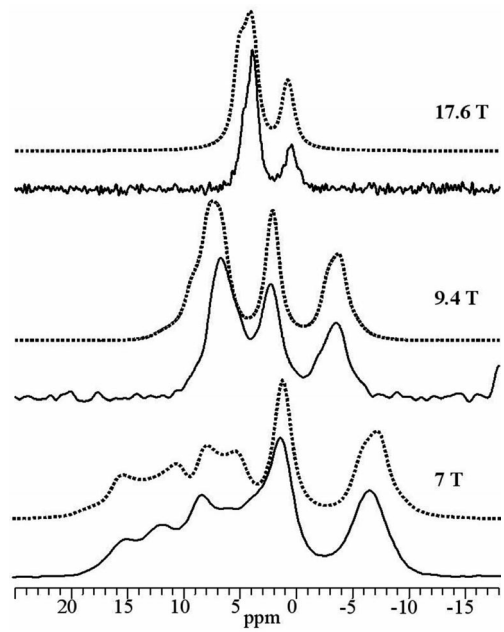

Figure 2. Experimental and simulated (dotted line) ^{29}Si CP/MAS NMR spectra of Ph_3SiBr at various B_0.

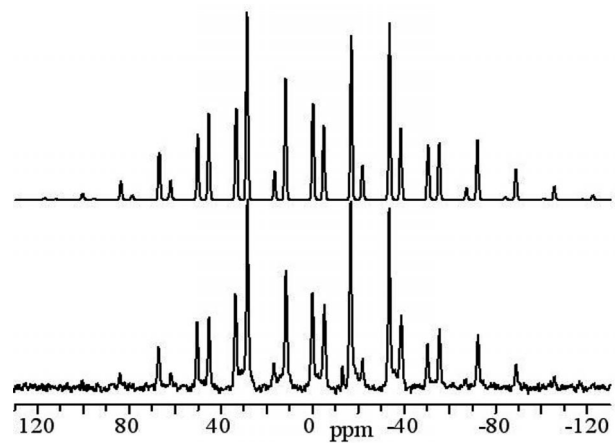

Figure 3. Experimental and calculated ^{29}Si CP/MAS NMR spectrum (above) of Ph_3SiF, ν_{rot} = 1 kHz.

Zeitschrift für anorganische und allgemeine Chemie ZAAC Journal of Inorganic and General Chemistry

and gave only minor changes in the spectra. Therefore, only one molecule was used to simulate the coupling pattern. In the simulation of the Ph_3SiCl spectrum both isotopes ^{35}Cl and ^{37}Cl were included in their natural abundance ratio. The simplifications may give rise to the slight differences between experimental and calculated spectra.

As can be seen from Figure 3, the SSB spectrum of Ph_3SiF reveals Si–F direct dipolar couplings. Thus, the shielding was extracted from the SSB spectrum using CSOLIDS,[12] which takes this parameter into account. The best match between experimental and simulated spectrum was achieved for δ_{11} = 10.7 ppm, δ_{22} = 5.7 ppm, δ_{33} = –24.3 ppm, and D = –5488 Hz (according to a Si–F distance of 1.6035(15) Å], ^1J(Si-F) was determined by solution NMR spectroscopy to be 282.1 Hz.

The principal components of the other triphenylsilane derivatives were extracted in a straightforward way (see Experimental section). Where the presence of different independent molecules in the crystallographic asymmetric unit caused severely overlapping signals in the SSB spectra (Ph_3SiOH, SH, Me), the RAI sequence (Recoupling of Anisotropy Interactions, vide infra) was applied for data acquisition. The measured and calculated isotropic chemical shifts and principal components of the shielding tensors together with the span Ω and the skew κ derived therefrom are listed in Table 2 and Table 3 for all Ph_3Si derivatives investigated (except Ph_3SiBr). Experimental δ, Ω and κ values are reported according to the Herzfeld-Berger convention.[15,16]

Table 2. Experimental (**bold**) and calculated components of the ^{29}Si shielding tensors of the investigated phenylsilanes (δ and Ω in ppm).

Compound		δ_{11}	δ_{22}	δ_{33}	δ_{iso}	Ω	κ
Ph_4Si*		**–6.6**	**–15.4**	**–17.6**	**–13.8**	**11**	**–0.6**
		–1.7	–18.9	–20.8	–13.8§	19.1	–0.8
Ph_3SiF[i]*		**10.7**	**5.7**	**–24.3**	**–2.6**	**35**	**0.7**
		20.8	5.9	–20.9	1.9	41.7	0.56
Ph_3SiOMe*		**7.2**	**–4.1**	**–44.7**	**–13.8**	**51.9**	**0.56**
	a	10.8	–3.4	–48.5	–13.7	59.3	0.52
		4.8	**–4.4**	**–33.3**	**–10.9**	**38.1**	**0.51**
	b	7.8	–0.2	–38.7	–10.4	46.5	0.66
Ph_3SiH*		**3.8**	**–14.4**	**–51.1**	**–20.6**	**54.9**	**0.34**
	[9]	**0.4**	**–13.2**	**–51.4**	**–21.1**	**51.8**	**0.46**
		8.3	–14.3	–54.8	–20.3	63.1	0.28
Ph_3SiMe*		**2.5**	**–12.**	**–19.9**	**–9.8**	**22.4**	**–0.3**
	a	4.4	–14	–19.4	–9.7	23.8	–0.54
		1	**–13.7**	**–17.8**	**–10.2**	**18.8**	**–0.56**
	b	2.3	–11.3	–20.4	–9.8	22.7	–0.2
Ph_3SiSH[ii]*		**13.5**	**–5.8**	**–11**	**–1.1**	**24.5**	**–0.57**
	a	25.6	–16.5	–24.2	–5.0	49.8	–0.69
		18.3	**–5.7**	**–17.3**	**–1.5**	**35.6**	**–0.35**
	b	30.2	–14.7	–31.8	–5.4	62	–0.44
$Ph_3SiCCPh$*		**–8.9**	**–35.2**	**–42.6**	**–28.9**	**33.6**	**–0.56**
	a	–12.5	–31.5	–43.2	–29.1	30.7	–0.24
		–12.8	**–32.1**	**–39.1**	**–27.8**	**26.9**	**–0.49**
	b	–10.4	–33.4	–40.3	–28.0	29.9	–0.54
Ph_3**Si**$SiMe_3$	[9]	**1.4**	**–32.2**	**–32.2**	**–21**	**33.6**	**–1**
		–12	–16.1	–29.6	–19.2	17.6	0.53
Ph_3Si**Si**Me_3	[9]	**–11.6**	**–11.6**	**–33.5**	**–18.9**	**21.9**	**+1**
		6.1	–23.5	–26.4	–14.6	32.5	–0.82
Ph_3SiNH_2		**–2.7**	**–14.7**	**–32.7**	**–16.7**	**30.2**	**0.2**
		10.7	–22.6	–28.7	–13.6	39.4	–0.68
$(Ph_3Si)_2$		**–2.2**	**–31.7**	**–39.5**	**–24.5**	**37.3**	**–0.58**
	[9]	**–1.8**	**–37.2**	**–37.2**	**–25.4**	**35.4**	**–1**
Ph_3SiCl		**18.9**	**0.33**	**–9**	**3.4**	**27.9**	**–0.33**

* Compounds selected for tensor discussion. $\delta_{iso} = (\delta_{11}+\delta_{22}+\delta_{33})/3$; $\Omega = \delta_{11}-\delta_{33}$ and $\kappa = 3(\delta_{22}-\delta_{iso})/\Omega$[16] [§] Experimental value used as reference, see Exp. Sect. [i] Principal components ± 5 ppm, Ω: ± 10 ppm, κ: ± 0.3. [ii] According to the crystal structure determined at 203 K.

Table 3. Experimental and calculated (a,b1–4) values of the ^{29}Si shielding tensor for Ph_3SiOH (δ and Ω in ppm), a and b represent the two tetrameric systems.

site	δ_{11}	δ_{22}	δ_{33}	δ_{iso}	Ω	κ
	3.3	–8.1	–26.1	–10.4	29.8	0.23
	2.6	–9.8	–26.8	–11.4	29.4	0.16
RAI	1.7	–7.3	–30.5	–12	32.2	0.44
RAI	5.7	–7.6	–35.5	–12.2	40.2	0.34
	5.3	–8.5	–37.5	–13.6	42.8	0.36
	9.4	–18.3	–36.6	–15.2	46	–0.21
	7.6	–10.6	–44	–15.7	51.6	0.3
a1	10.1	–4.9	–44.6	–13.2	54.7	0.45
a2	14.2	–3.6	–30.5	–6.6	44.7	0.2
a3	22.7	–11.8	–35.7	–8.3	58.4	–0.18
a4	7.9	–9.2	–32.8	–11.4	40.7	0.16
b1	20.5	–21.5	–39	–13.3	59.5	–0.41
b2	12	–10.9	–47.6	–15.5	59.6	0.23
b3	7.1	–8.7	–36	–12.5	43.1	0.26
b4	11.4	–6.2	–47.5	–14.1	58.9	0.4

Ph_3SiOH comprises eight independent molecules in the crystallographic asymmetric unit. Not all lines are resolved in the MAS spectrum. Two sites exhibit the same chemical shift at δ = –10.4 ppm, the signals at –12 and –12.2 ppm are superimposed (Figure 4). Measuring the shielding tensor by slow MAS decreases the resolution due to insufficiently averaged dipolar interactions. Within the RAI-sequence,[17] a MAS frequency fast enough to average disturbing interactions is applied, the anisotropy interactions are recoupled and are transferred into the second dimension. Using RAI the span and skew for the poorly resolved signals at about –12 ppm in Ph_3SiOH could be determined (Figure 4), whereas no separation was achieved for the signals at δ_{iso} = –10.4 ppm. Here the experimentally obtained average value is given.

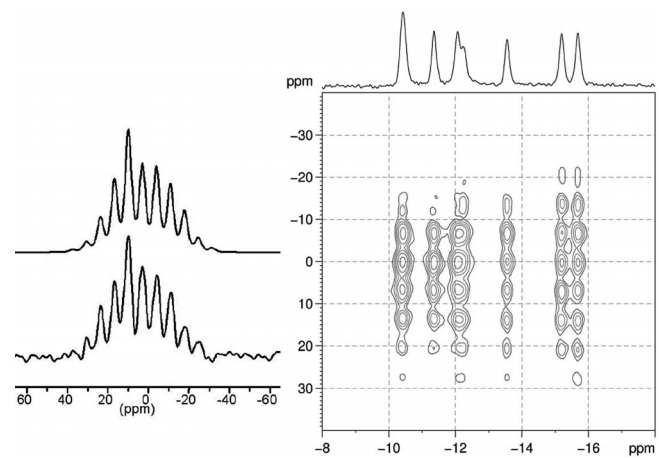

Figure 4. ^{29}Si RAI spectrum of Ph_3SiOH at ν_{rot} = 5 kHz together with one experimental (bottom) and simulated row (top) for extracting the principal components. On top of the 2D-plot the ^{29}Si CP/MAS NMR spectrum is shown.

DFT-IGLO Analyses

For the triphenylsilanes under investigation the principal components of the ^{29}Si shielding tensor were calculated using the DFT-IGLO method. The obtained data are listed in Table 2 and Table 3. For most compounds experimental and calculated data are in good accordance, but some striking discrepancies became obvious too. For the chloride and bromide system the calculated values show large differences to the experiment and are therefore not included. They are rationalized by the strong intermolecular effects due to the electrostatic interactions. It is well-known that molecular crystals, composed of polar molecules, have strong intermolecular interactions, such that the electron density of a molecule in the crystal is poorly approximated with a gas-phase model. As point charge models are usually not sufficient to correct for this deficiency and calculations of significantly higher sophistication would be required we decided to not quote the computational results at this place.

For the disilane $Ph_3SiSiMe_3$, the calculated isotropic chemical shift predicts the higher shielding for the phenyl-substituted silicon atom, as one would expect from chemical experience. Nevertheless, the span and skew rather fit to the $SiMe_3$ group and vice versa. Here the question arises whether the experimental assignment was misleading (our preferred interpretation, as the experimental chemical shift difference between the sites is only 2 ppm, well within the computational error margins, and the computed shielding tensor characteristics nicely match the experimental data of the alternative silicon atom in both cases).

Ph_3SiNH_2 shows larger differences for κ between experiment and calculation. This compound crystallizes in a kind of dimer with the NH_2 groups pointing to each other and one NH proton interacting with the neighboring nitrogen atom (d(NH) = 2.9 Å). Shielding tensor simulation of this dimer did not change the calculated κ significantly. Hydrogen dynamics and imprecisely defined hydrogen positions may contribute to this difference. As a result of the described discrepancies we decided not to consider Ph_3SiNH_2 and –$SiMe_3$ in the discussion of the principal component contributions.

Crystal Structures

The crystal structures of Ph_4Si,[18a–c] Ph_3SiH,[19] Ph_3SiNH_2,[20] $Ph_3SiSiMe_3$,[21] Ph_3SiSH,[22] Ph_3SiOH,[23] Ph_3SiCl,[24] and Ph_3SiMe[25a] have already been reported in the literature. Calculation for all Ph_4Si structures were carried out and gave only slightly differing results. The values given in Table 2 are those for the structure determined by *Parkanyi* et al.[18a]

Due to the lacking hydrogen positions in the structure of Ph_3SiSH new X-ray diffraction data sets were acquired (at 93 K and 203 K). The structure contains two independent molecules. At 203 K the position of one of the SH-hydrogen atoms was difficult to locate and two possible positions with site occupancies of 70 % (A1) and 30 % (A2) were refined. Shielding tensor calculations were performed for both conformers. Comparison with the experimental values showed a very good agreement when A1 position (with 70 % occupancy) is considered and completely different shielding for A2. In Table 2 the values for molecule A1 are given.

In addition to Ph_3SiSH, the structures of Ph_3SiF, Ph_3SiBr, Ph_3SiOMe and $Ph_3SiCCPh$ were determined in this work (Table 4). In the interim, *Bolte* et al. had published the structures of Ph_3SiMe and Ph_3SiBr.[25] Whereas the first is similar to the one obtained in our experiments, the latter was of poor quality (R-factor 9.4 %), thus reasoning the use of atomic coordinates from our X-ray diffraction experiments.

ORTEP diagrams of the compounds are given in Figure 5. With the exception of Ph_3SiF all compounds crystallize with two independent molecules in the asymmetric unit. For Ph_3SiMe, Ph_3SiOMe and $Ph_3SiCCPh$ the distinct resonances for both environments were resolved in the ^{29}Si NMR spectra. Unfortunately, it was impossible to obtain suitable crystals to solve the crystal structure of hexaphenyldisilane $(Ph_3Si)_2$. The compound crystallizes – irrespective of the solvent used – in very thin needles which appear to be severely twinned.

Discussion

As demonstrated in Table 2 and Table 3, the sets of experimental and calculated principal components are well in accord for most of the compounds. Smaller differences in the skew should not be overestimated. Due to the definition of the skew (see Table 2) for the small spans observed here, a slight change in δ_{22} has a great influence on κ. Another reason for differences between experimental and calculated values can be imperfections in the crystal structure data.

Tsantes et al.[26] studied the influence of the phenyl group rotation on the principal components in hexaphenylcyclotrisiloxane. In model calculations they found only minor influence on δ_{11} and δ_{33} (and therefore on Ω), but pronounced influence on δ_{22} resulting in large changes in κ.

The experimentally determined span seems to be systematically smaller than the corresponding calculated value. In addition to differences usually encountered between experiment and calculation, this can be due to the differences in temperature used in the NMR-experiment vs. X-ray structure determination, the latter being the basis for the calculations, as explained below in detail for the silanol example.

Although from the view point of the *ipso*-C atoms the Ph_3Si-group implies a C_3-axial symmetry on the first coordination sphere of the silicon atom, the values for the skew demonstrate that only very few tensors exhibit a κ value near 1 (or –1) and therefore an axial symmetry. Nevertheless, for most compounds κ is negative which means two directions of stronger shielding and component (11) representing a notably less shielded direction. Despite this seemingly systematic behavior of κ the directions of principal component (11) with respect to the Ph_3Si moiety vary within the set of compounds under investigation.

As examples molecules of Ph_3SiH, Ph_3SiOMe, Ph_3Si-CCPh, Ph_3SiMe and Ph_4Si are shown in Figure 6 with the directions of their calculated principal components of the ^{29}Si chemical shift tensor. The directions in Ph_3SiF are very similar to those

Zeitschrift für anorganische und allgemeine Chemie ZAAC Journal of Inorganic and General Chemistry

Table 4. Crystal data and structure refinement for Ph_3Si-Br, -F, -OMe, -SH and -CCPh.

Compound	Ph_3SiBr	Ph_3SiF	Ph_3SiOMe	Ph_3SiSH	Ph_3SiSH	$Ph_3SiCCPh$
Empirical formula	$C_{18}H_{15}BrSi$	$C_{18}H_{15}FSi$	$C_{19}H_{18}OSi$	$C_{18}H_{16}SSi$	$C_{18}H_{16}SSi$	$C_{26}H_{20}Si$
Formula weight	339.30	278.39	290.42	292.46	292.46	360.51
Temperature /K	173(2)	293(2)	293(2)	93(2)	203(2)	203(2)
Wavelength /Å	1.54180	1.54180	1.54180	0.71073	0.71073	0.71073
Crystal system	monoclinic	monoclinic	triclinic	monoclinic	monoclinic	monoclinic
Space group	$P2_1/c$	$P2_1/c$	$P\bar{1}$	$P2_1/c$	$P2_1/c$	$P2_1/c$
Unit cell dimensions						
a /Å	18.589(4)	10.243(2)	9.371(1)	18.5461(6)	18.6850(9)	12.8816(3)
b /Å	9.582(2)	11.623(2)	12.396(2)	9.5159(3)	9.6007(4)	11.3046(3)
c /Å	18.328(4)	13.299(3)	15.411(5)	18.2629(6)	18.3783(7)	28.6090(6)
α /°	90	90	70.98(2)	90	90	90
β /°	107.19(3)	109.78(3)	85.67(2)	107.657(1)	107.758(2)	101.326(1)
γ /°	90	90	76.16(2)	90	90	90
V /Å^3	3118.8(12)	1489.9(6)	1643.5(7)	3071.25(17)	3138.8(2)	4084.95(17)
Z	8	4	4	8	8	8
D_{calc} /Mg·m^{-3}	1.445	1.241	1.174	1.265	1.237	1.172
Absorption coefficient / mm^{-1}	4.206	1.368	1.215	0.276	0.270	0.122
F(000)	1376	584	616	1232	1232	1520
Crystal size /mm	0.35 × 0.30 × 0.30	0.25 × 0.20 × 0.18	0.62 × 0.58 × 0.50	0.55 × 0.40 × 0.35	0.50 × 0.20 × 0.10	0.60 × 0.50 × 0.20
θ-range for data collection /°	2.5–78.8	4.6–65.1	3.0–68.0	1.2–43.2	1.1–25.0	1.5–25.0
Index ranges	$-22 \le h \le 21$, $-11 \le k \le 0$, $0 \le l \le 22$	$-12 \le h \le 0$, $0 \le k \le 13$, $-14 \le l \le 15$	$-10 \le h \le 11$, $0 \le k \le 14$, $-17 \le l \le 18$	$-32 \le h \le 35$, $-18 \le k \le 16$, $-35 \le l \le 31$	$-22 \le h \le 22$, $-11 \le k \le 10$, $-21 \le l \le 21$	$-15 \le h \le 13$, $-13 \le k \le 13$, $-32 \le l \le 34$
Reflections collected	6084	2684	6269	84643	23275	33338
Independent reflections, R_{int}	5886, 0.0540	2532, 0.0222	5981, 0.0238	22866, 0.0250	5534, 0.0446	7201, 0.0286
Completeness to θ_{max} /%	99.4	99.5	99.7	99.4	100.0	100.0
Absorption correction	Psi-Scan	none	Psi-Scan	Semiempirical	Semiempirical	Semiempirical
max./ min. transmissions	0.2848, 0.2501		0.545, 0.496	0.9096, 0.8074	0.9735, 0.8769	0.9761,.8848
Data / restraints / parameters	5886 / 0 / 361	2532 / 0 / 181	5981 / 0 / 382	22866 /0 / 367	5534 / 3 / 370	7201 / 0 / 487
Final R indices [$I > 2\sigma(I)$]	R_1 = 0.0539, wR_2 = 0.1421	R_1 = 0.0437, wR_2 = 0.1072	R_1 = 0.0615, wR_2 = 0.1683	R_1 = 0.0348, wR_2 = 0.0947	R_1 = 0.0381, wR_2 = 0.0907	R_1 = 0.0366, wR_2 = 0.0954
R indices (all data)	R_1 = 0.0706, wR_2 = 0.1499	R_1 = 0.0617, wR_2 = 0.1161	R_1 = 0.0754, wR_2 = 0.1744	R_1 = 0.0526, wR_2 = 0.1049	R_1 = 0.0689, wR_2 = 0.1001	R_1 = 0.0509, wR_2 = 0.1010
Goodness-of-fit on F^2	1.077	1.082	1.143	1.030	1.045	1.083
Largest diff. Peak & hole /e·Å^{-3}	1.029, –0.856	0.337, –0.271	0.346, –0.357	0.637 –0.417	0.243, –0.272	0.246, –0.236

in the methoxy- and methylsilane and therefore not shown here. For compounds having two molecules in the asymmetric unit only one of them is depicted. (The differences between the independent molecules with respect to the directionality of the principal components are small and do not show a qualitatively different result.)

For $Ph_3SiCCPh$ and Ph_3SiOMe one principal component is nearly pointing along the Si–*R* axis. In the first, however, strongest shielding can be found in the direction of the phenyl groups, whereas the direction Si–*R* (to the acetylene substituent) is less shielded.

For Ph_3SiOMe the observed span and skew are very similar to those determined by *Harris* et al.[9] for $Ph_3SiOSiPh_3$ (δ_{iso} = –17 ppm, Ω = 34.1 ppm, κ = 0.3). The strongest shielding is observed in the direction of the OMe substituent. In the direction of the phenyl groups, silicon is less shielded. If we consider the contributions of the Si–*R* bonds to the principal components (Table 5) it becomes obvious, that the component pointing in the direction of *R* is always that one having the lowest deshielding contribution.

A seemingly similar situation is observed for Ph_3SiMe (component (33) pointing almost along the Si–Me axis), but the significantly narrowed span (with respect to the former two compounds) and the slight deviation of (33) from the Si–Me axis already hints at less pronounced differences between Ph and Me in the influence on the shielding tensor, the summit being four Ph groups (in $SiPh_4$) resulting in a very narrow span and all principal components pointing in between the Si–C bond axes (as expected for a tetrahedral system aligned within the orthogonal axes of a coordinate system). In Ph_3SiSH the strongest and lowest shielding components are found in the phenyl group plane (whereas δ_{22} points to the substituent SH), and Ω (its components being located within the Ph_3Si plane) amounts to 24.5 and 35.6 ppm. In Ph_3SiH the skew differs much from being axial, although the Si–H bond should exert radial symmetric (*de*)shielding influence within the SiC_3 plane.

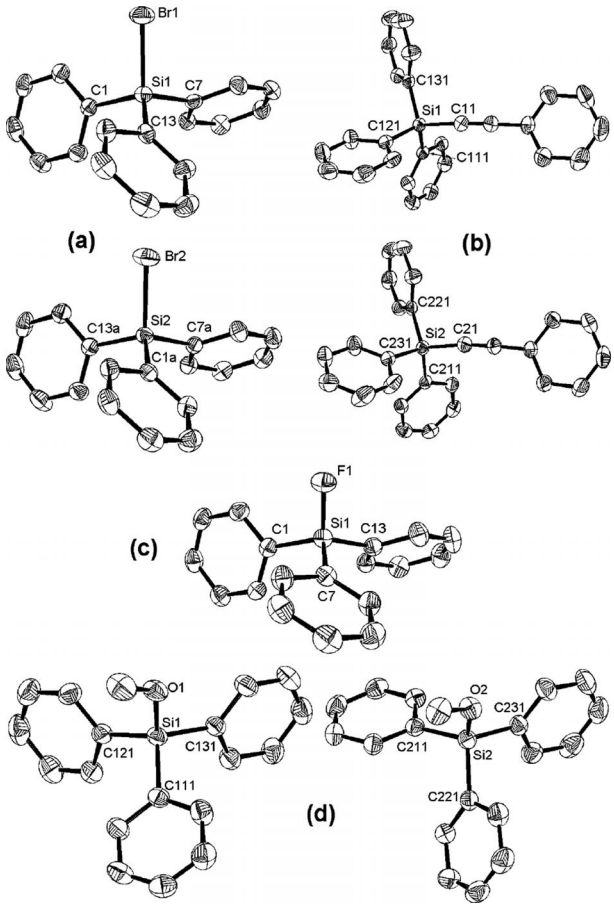

Figure 5. Molecular structures of a) Ph_3SiBr, b) $Ph_3SiCCPh$, c) Ph_3SiF d) Ph_3SiOMe, 50 % and 30 % (d) -ellipsoids, both molecules of the asymmetric unit shown for a, b and d.

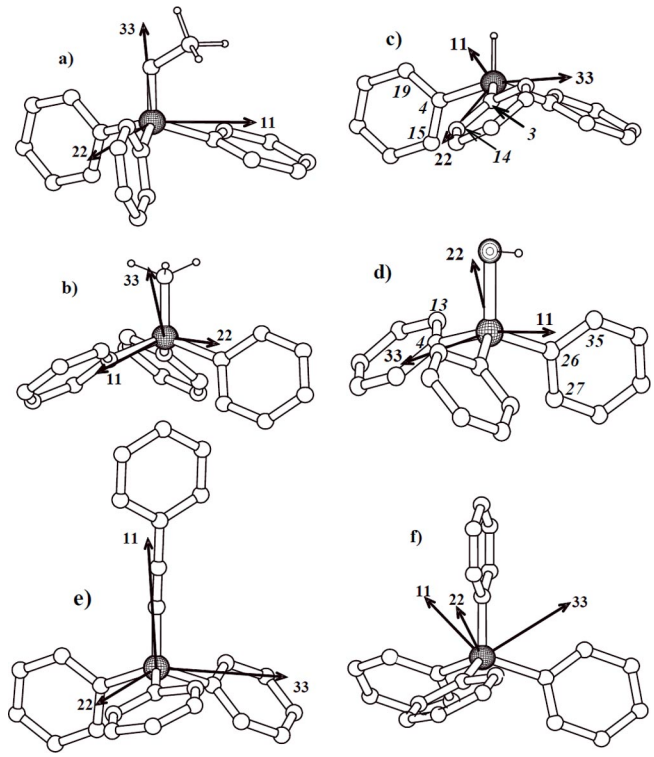

Figure 6. Calculated orientation of the principal components in various triphenylsilanes, hydrogen atoms at phenyl have been omitted a) Ph_3SiOMe b) Ph_3SiMe c) Ph_3SiH d) Ph_3SiSH e) $Ph_3SiC{\equiv}CPh$ f) Ph_4Si.

δ_{33} is directed between two of the Si–C bonds, again exerting highest shielding within the idealized $SiPh_3$ plane, but this time without one of the components (11) or (22) pointing along the Si–*R* axis. Hence, these directions cannot only be determined by the mere presence of the substituent *R* as the predominant influence, becoming particularly obvious in case of Ph_3Si–H with a radial symmetric Si–H σ bond which should exert equal influence on all directions in the perpendicular plane. Further analyses of the contributions of each substituent on the shielding were thus necessary.

Looking at the deshielding contributions calculated by DFT-IGLO the main contribution are of course those of the direct bonds. Bonding orbitals other than the Si–*R* and Si–Ph bonds, lone pairs of the substituent (if present), and second neighbor effects (e.g. *ortho*-C) – are smaller by nearly two orders of magnitude. All others are inconsiderable. Concerning the share of the phenyl groups and substituents *R* (Table 6) it can be observed that with increasing electronegativity of the substituent the deshielding contribution of the substituent is reduced. At the same time the contribution of the phenyl groups (except for *R* = C≡CPh, where the contribution is similar to compounds with substituents having a Si–C bond) is increased, the sum of these contributions mainly determines δ_{iso}.

Table 5. LMO contributions to σ in principal axes in ppm. For atom numbers see italics in Figure 6.

R	Contribution	11	22	33
H	bond H–Si	–60.4	–88.1	–139.2
	bond H35–C19	–2.2	–3.6	–0.3
	bond C4–C15	–4.1	–5.3	–1.5
	bond C4–C19	–3.5	–4.3	–1.2
	bond C3–C14	–7.4	–1.3	–1.6
SH (B)	bond S–Si	–149.4	–0.9	–136.6
	AO S	–4.2	3.3	–1.2
	bond C26–C35	–7.2	–1.3	–1.6
	bond C26–C27	–3.4	2.5	–0.9
	bond Si–C4	–2.9	–148.9	–161.4
OMe	bond O–Si	–138.5	–130.5	4.5
Me (A)	bond Si–CH_3	–160.0	–177.5	–16.4
OH (B1)	bond O–Si	–151.5	–115.3	4.1
	bond O–H	–3.2	–6.6	5.5
	bond C4–C12*	–6.6	–1.4	–1.3
(B4)	bond O–Si	–140.2	–121.5	–4.8
	bond O–H	–2.7	–5.8	4.9
	bond C5–C21*	–6.2	–1.1	–1.2
CCPh	bond Si–C(CPh)	–1.8	–101.6	–97.5
	bond C≡C	1.4	–10.6	–18.6

A similar trend can partially be observed for the anisotropy. *Radeglia* et al. already pointed out for SiO_4 environments that the span increases with increasing differences in bond polarity between the four substituents at silicon.[27] These effects should mainly contribute to the observations according to our initial model, i.e., the shielding along the Si–*R* axis being dif-

Zeitschrift für anorganische und allgemeine Chemie ZAAC Journal of Inorganic and General Chemistry

Table 6. Average Ph and *R* deshielding contributions calculated by IGLO. * = deshielding contribution of the Si–*R* bond corrected for the bond orbital and lone pair contributions of the *R* substituent.

substituent	average Ph contribution /ppm	*R* contribution* /ppm	δ_{iso} /ppm
F	–123.6	–60.8	1.9
C≡CPh	–103.1	–67	–29.1
OMe	–113.1	–75.6	–13.7
	–113.5	–75.6	–10.4
OH	–112.8	–77,8	–13.2
	–114.8	–77.4	–6.6
	–114	–78.6	–8.3
	–113.7	–76.4	–11.4
	–112.8	–75.7	–13.3
	–112.4	–75.2	–15.5
	–113.4	–75.6	–12.5
	–113.2	–75.8	–14.1
SH	–107.8	–94.2	–5.05
	–107.4	–95.3	–5.45
H	–101.7	–95.6	–20.3
Ph	–100	–100	–13.8
Me	–98	–118	–9.7
	–98	–117	–9.8

ferent from the shielding within the SiC_3 plane, whereas within the latter only small differences should be found (in above examples up to ca. 10 ppm). Pronounced differences in shielding within the SiC_3 plane, however, must be the result of further intra- and intermolecular interactions which imply directed influence on the deshielding contributions. One such directing influence should be the bond angle Si–*R*–*Y* (e.g., Si–O–H, Si–S–H, Si–O–Me), another one should result from the relative orientation of the phenyl planes with respect to the Si–*R* bond, and further effects might arise from intermolecular forces. Thus, the influence of Si–*R*–*Y* bond angle orientation and the positioning of phenyl planes relative to the Si–*R* axis were further analyzed.

For Ph_3SiH the pronounced shielding along (33) within the SiC_3 plane and the effect that none of the main axes is pointing along the substituents could only arise from effects of the relative Ph-orientation. Whereas the three Si–C bonds exert similar deshielding influence with respect to their effect on δ_{iso}, the phenyl plane at C4 is nearly parallel to the Si–H bond, thus hinting at attractive force between the Si-bound (and thus hydridic) hydrogen atom and an *ortho*-CH. Indeed, the bond angle H–Si–C4 is smaller for this group (106.8° vs. 108.5°/ 108.6° for the other H–Si–C). A directing influence of this particular phenyl group on the shielding tensor may thus be expected. This directing influence is particularly based on effects of the ortho CH bond and the two ortho CC bonds, which have significant isotropic contributions and, in particular, exert pronounced deshielding along (11) and (22), whereas direction (33) remains well shielded (see Table 5). Although these values are small, they contribute to the span of 54.9 ppm by 6.7 ppm. A further contribution of similar nature is generated by an ortho CC bond of phenyl group at C3 which exerts pronounced deshielding along (11), thus contributing to the span with 5.8 ppm. All other ortho carbon bonds show contributions of similar size to all main axes. It should be mentioned that in Ph_3SiF similar effects concerning the F–Si–C angles and contributions of ortho phenyl carbon atoms can be found.

In Ph_3SiSH the Si–S axis is close to the direction of principal component (22), thus making analysis of significant contributions to (11) vs. (33) (almost within the SiC3 plane) appear worthwhile. The most obvious directing influence, the S–H bond, does not exhibit any relevant differentiation between (11) and (33). The direction of the S-located atomic orbital (AO), however, also depends on the directions of the S–H bond, and indeed the S-AO contribution exerts pronounced deshielding in direction (11), whereas direction (33) is less influenced by the same (Table 5). With respect to the directional influences of the phenyl groups, the Si-C4 bond of the phenyl ring, which mainly effect (33) appear less deshielding with respect to its isotropic influence (–104.3 vs. –107.8 and –110 ppm for the other Si–C bonds). Furthermore, an effect of the orientation of the phenyl planes can be found (as for Ph_3SiH) arising from the phenyl groups which are almost parallel to the Si–S bond (C26 to C35 and C27).

Several compounds exhibit two or more molecules in the asymmetric unit. An assignment of the observed chemical shifts to the molecules in the crystal structure was possible for $Ph_3SiCCPh$, Ph_3SiOMe, Ph_3SiSH and Ph_3SiMe, although for the latter two the experimental differences are smaller than the calculation error bars and the assignment should be handled with care. In most cases the differences between the principal components of the molecules are small. Examining the deshielding contributions given in the calculation not a single one can be attributed to the differences in the principal components of the two molecules in the asymmetric unit, it is an effect of several contributions from bond length and angle variations as a result of crystal packing.

Due to the fact that the differences in δ_{iso} and Ω between the two crystallographically independent molecules are larger than for the other compounds Ph_3SiOMe was examined in more detail. A comparison of the crystal structure for both molecules shows very similar bond lengths and angles except for the dihedral angles describing the phenyl group orientation with respect to the Si–O bond (molecule a: 73.9°, 2.27°, 8.11°; b: 78.56°, 38.34°, 11.44°) and the orientation of the OMe group (a: 51.2°, b: 58.2°). Considering the calculated contributions to the principal axis it can be observed that the differences in span mainly – but not exclusively – can be attributed to the Si–O bond, which show larger differences in the 11 and 33 components for molecule **a** (–138.5 and +4.5 ppm, –133.9 and +1.4 ppm for **b**), in contrast to the less pronounced differences in contributions of the Si–C bonds.

Ph_3SiOH proved to be a very interesting compound, due to the hydrogen bridge system formed between the silanol groups the crystal structure is built of two ring-like systems consisting of four molecules each, Figure 7.

The calculations reflect the trend in the experimental values: (i) the span increases with increasing shielding of the sites and (ii) the change in Ω is mainly due to changes in δ_{33}. Only one experimental site shows a negative κ, all others have a positive. The smaller experimental than calculated span we attribute to the fact that the X-ray structure was recorded at 123

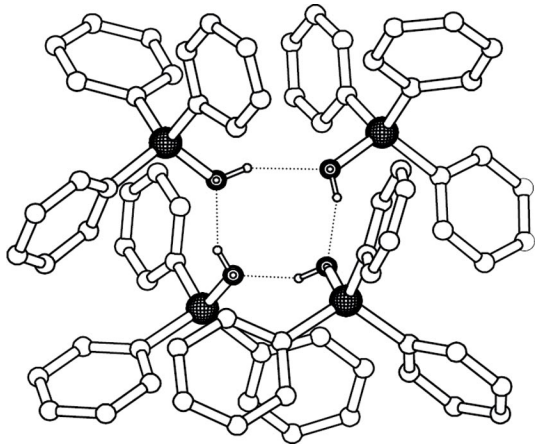

Figure 7. Part of the crystal structure of Ph_3SiOH.[23] Only one of the two tetramer rings is shown. Hydrogen atoms at the phenyl substituent are omitted.

K,[23b] whereas the NMR measurements were performed at 295 K. There is a dynamic hydrogen bond rearrangement within the tetrameric ring systems,[28] which will be frozen below 258 K. Unfortunately, it was not possible to repeat the tensor measurements at low temperature with our equipment, because all Ph_3SiR except R = Alkyl had a poor CP-efficiency and very long T_1(H).

Figure 8 shows two example molecules of ring system b with the calculated directions of the principal components, including **b1** having the only negative κ in experiment. The molecules mainly differ in the orientation of the phenyl planes relative to the Si-O-bond, in the O–Si–C angles and in the orientation of the OH-group with respect to the Si–C bonds. The influence of the phenyl orientation on the shielding was already mentioned above.[26]

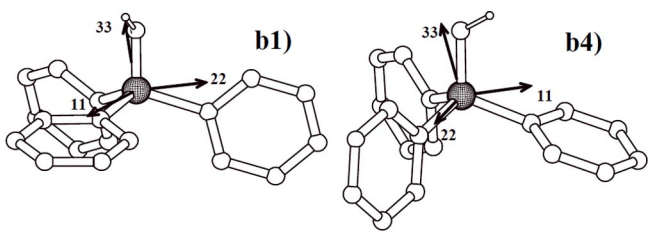

Figure 8. Calculated orientation of the principal components in Ph_3SiOH-molecules b1 and b4, Hydrogen atoms at the phenyl substituent are omitted.

Regarding the contributions of the different bonds (Si–C, Si–O) and lone pair (O) orbitals calculated by IGLO the differences in κ, Ω and δ_{iso} are again the sum of several influences. Si–O and O–H-contributions are directing the strongest shielding towards the OH-substituent. With respect to the crystal structure it is worth pointing out that the two molecules with the negative calculated skew **b1** and **a3** have the smallest dihedral angle H–O–Si–C with 13.04° for **b1** (in comparison to 23.08°, 28.73° and 47.83° for **b2–4**) and 19.6° for **a3** (in comparison to 26.41°, 44.97° and 45° for **a1,2,4**) which means the OH proton nearly points in the direction of one C–Si–O-plane in **b1**.

The directing influence of the OH bond becomes obvious for the Si–O bond, which exerts pronounced deshielding along (11) although both (11) and (22) are almost perpendicular to the Si–O bond axis, see Table 4. This effect is particularly pronounced for those silanol molecules with a small dihedral angle between the OH bond and direction (11) – as for **b1**. Directing influences of some ortho C–C bonds in phenyl groups, shown for the example molecules in Table 5, add further contributions to the difference between (11) and (22).

Conclusions

Chemical shift anisotropy tensors were measured and calculated for a series of substituted triphenylsilanes. For substituents containing quadrupolar nuclei residual dipolar couplings could be observed and coupling constants estimated therefrom.

For most compounds the calculations are, despite the small observed spans, in very good accordance with the experimental results. Especially for Ph_3SiOH even the small variations in span and skew could be reproduced by the calculations and explained by the derived contributions.

In several compounds having two molecules in the asymmetric unit ($Ph_3SiCCPh$, Ph_3SiOMe and Ph_3SiSH) the good representation of the measured values by the calculation allows the assignment of the NMR signals to a distinct molecule within the structure and therefore a discussion of the influence of the crystallographic differences on the chemical shift values.

Both experimental and calculated principal components demonstrate that beside the nature of the substituents crystal packing effects due to phenyl arrangement and hydrogen bonding have large influence on the principal components of the chemical shift tensor. Contrary to many silicon coordination compounds the changes in shielding cannot be attributed to a single predominant change in bond angle or length but are a summarized effect of several contributions. Within the small spans of the tensors in fourfold coordinated Ph_3Si-derivatives the detailed consideration of the LMO-contributions showed that the comparatively small differences in the molecular architecture (caused by packing and hydrogen bonding effects) have a much larger influence on the shielding tensor shape (in particular κ) than in most of the hypercoordinated silicon complexes exhibiting much larger spans [5a–i].

Especially in case of triphenylsilanol the various influences of the substituents, their orientation towards the Si-C-bonds of the phenyl groups, the influence of phenyl ortho CC bonds, as particular deshielding of (11) depending on the parallel or orthogonal arrangement of the Ph group relative to the SiO bond, it becomes obvious that various subtle contributions add to the final directionality, size and shape of the shielding tensor. Thus the consideration of the LMO-contributions gives interesting insights into the origins of chemical shift effects in silicon compounds.

The effect of the varying substituents hydrogen orientation on the skew in systems capable of hydrogen bonding as observed for the silanol could also be an explanation for the difference in experimental and calculated κ for the Ph_3SiNH_2-molecule, despite the fact that δ_{iso} and Ω are in satisfying

Zeitschrift für anorganische und allgemeine Chemie ZAAC Journal of Inorganic and General Chemistry

agreement. In case that the hydrogen position is not correctly determined or influenced by dynamic processes this will contribute noticeably to differences in experimentally observed and calculated values. The same reason may be considered for the fact that in Ph_3SiOH and Ph_3SiSH the measured anisotropies are smaller than the calculated.

Experimental Section

Triphenylsilanes: Ph_3SiH, Ph_3SiCl, Ph_3SiF, Ph_3SiSH, Ph_3SiNH_2, Ph_3SiMe, Ph_4Si, (Fluka, ABCR), Ph_3SiOH and $(Ph_3Si)_2$ (Wacker) were used as obtained. X-ray quality single crystals of Ph_3SiMe and Ph_3SiF were crystallized from toluene, Ph_3SiSH from toluene/n-hexane. All other silanes were synthesized under dry argon using standard Schlenk techniques according to *Soundararajan* et al.[29] (Ph_3SiBr), *Selina* et al.[30] ($Ph_3SiC{\equiv}CPh$), and *Sormunen* et al.[31] (Ph_3SiOMe).

^{29}Si CP/MAS measurements were carried out with Bruker MSL 300, AVANCE 400 WB (Ph_3SiBr, Ph_3SiCl, Ph_3SiF and RAI spectra), and Bruker Avance 750 WB spectrometers (Ph_3SiBr) with tppm15 decoupling. At 7 and 9.4 T, a 7 mm CP/MAS probehead and at 17.6 T, a 4 mm CP/MAS probehead was used. The ^{29}Si chemical shift was referenced using the high-field signal of the Q^4- groups in Q_8M_8 (δ = –109 ppm with respect to TMS = 0 ppm).

Samples were positioned in the middle of the ZrO_2 rotors using Kelf inserts or Cramps rotors. Slow spinning rates were stabilized by introducing a reducing valve into the drive pressure line. The number of spinning sidebands for tensor evaluation was adjusted to an optimum value recommended by *Hodgkinson* and *Emsley*.[32] The principal components of the shielding tensor were calculated from spinning sideband spectra using the programs DMFIT[33] and HBMAS (D. Fenzke, Universität Leipzig, 1989). Tensor orientation was inserted into the crystal structure using COSMOS®[34].

X-ray diffraction data were recorded with an ENRAF-NONIUS-CAD4-diffractometer (with spot detection by scintillation counter) using Cu-K_α-radiation (Ph_3SiBr, Ph_3SiF, Ph_3SiOMe) as well as with a BRUKER-SMART-CCD-diffractometer (Ph_3SiMe) or with a BRUKER-NONIUS-X8 APEXII-CCD-diffractometer (Ph_3SiSH, $Ph_3SiCCPh$) with Mo-K_α-radiation. The structures were solved with direct methods and refined with full-matrix least-squares methods. All non-hydrogen atoms were refined anisotropically. Hydrogen atoms were isotropically refined in idealized positions using a riding model (Ph_3SiBr, Ph_3SiF, Ph_3SiOMe, $Ph_3SiCCPh$, phenyl-H in Ph_3SiSH), localized by residual electron density (Ph_3SiMe) or localized on residual electron density maps and refined using a riding model (S–H in Ph_3SiSH at 93 K) as well as bond length restraints (distance S–H in Ph_3SiSH at 203 K fixed: 1.20 Å). For one of the two crystallographically independent molecules in the structure of Ph_3SiSH at 203 K two disordered sites of the S-bonded hydrogen atom were detected and refined in a site occupation ratio 70 % / 30 %. Structure solution and refinement of F^2 against all reflections were performed with SHELXS-97 and SHELXL-97 (G.M. Sheldrick, Universität Göttingen, 1986–1997).

Crystallographic data (excluding structure factors) for the structures reported in this paper have been deposited with the Cambridge Crystallographic Centre as supplementary publication numbers CCDC-621567 ($Ph_3SiC{\equiv}CPh$), CCDC-621568 (Ph_3SiF), CCDC-621569 (Ph_3SiMe), CCDC-621570 (Ph_3SiOMe), CCDC-621571 (Ph_3SiSH, 203 K), CCDC-621572 (Ph_3SiSH, 90 K), and CCDC-621573 (Ph_3SiBr). Copies of the data can be obtained on application to CCDC, 12 Union Road, Cambridge CB2 1EZ, UK. (Fax: +44-1223/336-033; E-mail: deposit@ccdc.cam.ac.uk).

Calculations: The molecular crystals have been approximated as individual molecules or as clusters of molecules. Initial geometries have been taken from the X-ray diffraction analysis, and partially reoptimized at the B3LYP/6-31G* level as implemented in Gaussian 03.[35] During optimization all intermolecular distances, the bond lengths between silicon and its non-hydrogen neighboring atoms as well as the orientation of all bonds and dihedrals in the molecules or clusters were kept frozen. NMR shielding tensors have been computed at the PBE/IGLO-III level for the reoptimized geometries[36a,b] using deMon2K[37]. NMR shielding tensor calculations employed the individual-gauge for local orbitals (IGLO) method [38] on the localized PBE/IGLO-III molecular orbitals[39]. All shielding calculations have been carried out using the MASTER code[40]. Chemical shifts have been calculated with respect to those of tetraphenylsilane (TPS, δ_{iso} = –13.8 ppm), and have then be converted to chemical shifts with respect to tetramethylsilane (TMS) using the conversion δ_{TMS} (X) = δ_{TMS} (TPS) + σ(TPS) – σ(X). Here, the chemical shift of TPS with respect to TMS is taken from experiment. Intermolecular effects, which have been found to be essential for molecular crystals containing aromatic rings,[41] have been included by the direct evaluation of molecular clusters of one molecule and its next neighbors.

Acknowledgments

The authors thank *Dr. C. Notheis* for preliminary work on Ph_3SiH, –NH_2 and –Cl. We also gratefully acknowledge *Dr. R. Lehnert* (Wacker) for providing samples of Ph_3SiOH and $[Ph_3Si]_2$, *Dr. A. Pampel* (Universität Leipzig) for performing the ^{29}Si MAS measurement of Ph_3SiBr at 17.6 T, *Professor Klaus Eichele* from Tübingen for providing CSOLIDS and WSOLIDS and *Professor B. Thomas* for performing the calculation of the Ph_3SiF-spinning side band spectrum using CSOLIDS.

References

[1] a) E. A. Williams, in: *The Chemistry of Organic Silicon Compounds* (Ed.: S. Patai, Z. Rappoport), John Wiley & Sons, **1989**, pp. 511; b) Y. Takeushi, T. Takayama in *The Chemistry of Organic Silicon Compounds* (Ed.: Y. Apeloig, Z. Rappoport), John Wiley & Sons, **1998**, pp. 267.

[2] H. Marsmann, *NMR – Basic Principles and Progress – 17: ^{29}Si NMR Spectroscopic Results*; Springer, Berlin, **1982**, pp. 65.

[3] F.Uhlig, U.Hermann, H. Marsmann, *^{29}Si NMR Database*, http://www.silicium-nmr.tugraz.at, 4.5.**2011**.

[4] J. C. Facelli, *Prog. Nucl. Magn. Reson. Spectrosc.* **2011**, *58*, 176–201.

[5] a) G. W. Fester, J. Eckstein, D. Gerlach, J. Wagler, E. Brendler, E. Kroke, *Inorg. Chem.* **2010**, *49*, 2667; b) D. Schöne, D. Gerlach, C. Wiltzsch, E. Brendler, T. Heine, E. Kroke, J. Wagler, *Eur. J. Inorg. Chem.* **2010**, *3*, 461; c) E. Brendler, T. Heine, A. F. Hill, J. Wagler, *Z. Anorg. Allg. Chem.* **2009**, *635*, 1300; d) G. W. Fester, J. Wagler, E. Brendler, U. Böhme, D. Gerlach, E. Kroke, *J. Am. Chem. Soc.* **2009**, *131*, 6855; e) G. W. Fester, J. Wagler, E. Brendler, U. Böhme, G. Roewer, E. Kroke, *Chem. Eur. J.* **2008**, *14*, 3164; f) D. Gerlach, E. Brendler, T. Heine, J. Wagler, *Organometallics* **2007**, *26*, 234; g) J. Wagler, U. Böhme, E. Brendler, S. Blaurock, G. Roewer, *Z. Anorg. Allg. Chem.* **2005**, *631*, 2907; h) J. Wagler, U. Böhme, E. Brendler, B. Thomas, S. Goutal, H. Mayr, B. Kempf, G. Ya. Remennikov, G. Roewer, *Inorg. Chim. Acta* **2005**, *358*, 4270; i) R. Bertermann, A. Biller, M. Kaupp, M. Penka, O. Seiler, R. Tacke, *Organometallics* **2003**, *22*, 4104.

[6] M. G. Gibby, A. Pines, J. S. Waugh, *J. Am. Chem. Soc.* **1972**, *94*, 6231.
[7] a) J. D. Cavalieri, R. West, J. C. Duchamp, K. W. Zilm, *J. Am. Chem. Soc.* **1993**, *115*, 3770; b) R. West, J. D. Cavalieri, J. C. Duchamp, K. W. Zilm, *Phosphorus Sulfur Silicon Relat. Elem.* **1994**, *213*, 93; c) K. W. Zilm, D. M. Grant, J. Michl, M. J. Fink, R. West, *Organometallics* **1983**, *2*, 193; d) V. Kravchenko, R. Kinjo, A. Sekiguchi, M. Ichinohe, R. West, Y. S. Balazs, A. Schmidt, M. Karni, Y. Apeloig, *J. Am. Chem. Soc.* **2006**, *128*, 14472.
[8] J. D. Epping, S. Yao, M. Karni, Y. Apeloig, M. Driess, *J. Am. Chem. Soc.* **2010**, *132*, 5443.
[9] R. K. Harris, T. N. Pritchard, E. G. Smith, *J. Chem. Soc. Faraday Trans. 1* **1989**, *85*, 1853.
[10] L. Mäler, L. di Bari, J. Kowalewski, *J. Phys. Chem.* **1994**, *98*, 6244.
[11] a) E. Brendler, Ch. Notheis, B. Thomas, *21st National Meeting FG Magnetic Resonance GdCh*, Würzburg, Germany, September 29–October 02, **1999**; b) E. Brendler, R. Witter, Th. Heine, *4th Alpine Conference on Solid State NMR* Chamonix, France, September 11–15, **2005**; c) R. J. Iuliucci, J. M. Fidler, G. T. Burg, *4th Alpine Conference on Solid State NMR* Chamonix, France, September 11–15, **2005**; d) G. T. Burg, R. J. Iuliucci, *229th ACS National Meeting*, San Diego, CA, USA, March 13–17, **2005**; e) R. J. Iuliucci, K. T. Mueller, *236th ACS National Meeting*, Philadelphia, PA, USA, August 17–21, **2008**.
[12] a) K. Eichele, *CSOLIDS*; *WSOLIDS*, Solid-State NMR Spectrum Simulation, http://casgm3.anorg.chemie.uni-tuebingen.de/klaus/soft/_index.html, Universität Tübingen, Germany, **2007**; b) K. Eichele, R. E. Wasylishen, *Inorg. Chem.* **1994**, *33*, 2766; c) K. Eichele, R. E. Wasylishen, J. S. Grossert, A. C. Olivieri, *J. Phys. Chem.* **1995**, *99*, 10110; d) B. Thomas, S. Paasch, S. Steuernagel, K. Eichele, *Solid State Nucl. Magn. Reson.* **2001**, *20*, 108.
[13] K. B. Dillon, R. J. Lynch, Th. C. Waddington, *J. Chem. Soc. Dalton Trans.* **1973**, 1478.
[14] E. Schempp, M. Chao, *J. Phys. Chem.* **1976**, *80*, 193.
[15] J. Herzfeld, A. E. Berger, *J. Chem. Phys.* **1980**, *73*, 6021.
[16] J. Mason, *Solid State Nucl. Magn. Reson.* **1993**, *2*, 285.
[17] R. Witter, St. Hesse, U. Sternberg, *J. Magn. Reson.* **2003**, *161*, 35.
[18] a) L. Parkanyi, K. Sasvari, *Period. Polytech. Chem. Eng.* **1973**, *17*, 271; b) C. Glidewell, G. M. Sheldrick, *J. Chem. Soc. A* **1971**, 3127; c) V. Gruhnert, A. Kirfel, G. Will, F. Wallrafen, K. Recker, *Z. Kristallogr. Kristallgeom. Kristallphys.* **1983**, *163*, 53.
[19] J. Allemand, R. Gerdil, *Cryst. Struct. Commun.* **1979**, *8*, 927.
[20] K. Ruhlandt-Senge, R. A. Bartlett, M. N. Olmstead, Ph. P. Power, *Angew. Chem.* **1993**, *105*, 459.
[21] L. Parkanyi, E. Hengge, *J. Organomet. Chem.* **1982**, *235*, 273–76.
[22] R. Minkwitz, A. Kornath, H. Z. Preut, *Z. Anorg. Allg. Chem.* **1993**, *619*, 877.
[23] a) H. Puff, K. Braun, H. J. Reuter, *J. Organomet. Chem.* **1991**, *409*, 119; b) M. Nieger, *Cambridge Crystallographic Structural Database* CCDC-163617, Private Communication, **2001**.
[24] E. B. Lobkowski, W. N. Fokin, K. N. Semenenko, *J. Struct. Chem.* **1981**, *22*, 152.
[25] a) T. Kückmann, H.-W. Lerner, M. Bolte, *Acta Crystallogr., Sect. E* **2005**, *61*, 3030; b) H. Steinert, H.-W. Lerner, M. Bolte, *Acta Crystallogr., Sect. E* **2008**, *64*, 880.
[26] G. Tsantes, N. Auner, T. Müller, A. R. Grimmer *Solid State NMR of Hexaphenylcyclotrisiloxane: An Unusual View on a Bulk Material*, 22nd Discussion Meeting, Progress in the Magnetic Resonance of Bioactive Compounds and New Materials, Regensburg, Germany, September 27–30, **2000**.
[27] R. Radeglia, A. R. Grimmer, *Z. Phys. Chem. (Leipzig)* **1981**, *262*, 718.
[28] A. E. Aliev, C. E. Atkinson, K. D. M. Harris, *J. Phys. Chem. B* **2002**, *106*, 9013.
[29] R. Soundararajan, D. S. Matteson, *Organometallics* **1995**, *14*, 4157.
[30] A. A. Selina, S. S. Karlov, E. V. Gauotchenova, A. V. Churakov, L. G. Kuzmina, J. A. K. Howard, J. Lorberth, G. S. Zaitseva, *Heteroat. Chem.* **2003**, *15*, 43.
[31] P. Sormunen, E. Iiskola, E. Vahasarja, T. T. Pakkanen, *J. Organomet. Chem.* **1987**, *319*, 327.
[32] P. Hodgkinson, L. Emsley, *J. Chem. Phys.* **1997**, *107*, 4808.
[33] D. Massiot, F. Fayon, M. Capron, I. King, S. Le Calvé, B. Alonso, J. O. Durand, B. Bujoli, Z. Gan, G. Hoatson, *Magn. Reson. Chem.* **2002**, *40*, 70.
[34] U. Sternberg, F. T. Koch, P. Losso, http://www.cosmos-software.de/co_intro.html, 2.5.**2011**.
[35] *Gaussian 03*, Revision C.02, M. J. Frisch, G. W. Trucks, H. B. Schlegel, G. E. Scuseria, M. A. Robb, J. R. Cheeseman, J. A. Montgomery Jr., T. Vreven, K. N. Kudin, J. C. Burant, J. M. Millam, S. S. Iyengar, J. Tomasi, V. Barone, B. Mennucci, M. Cossi, G. Scalmani, N.Rega, G. A. Petersson, H. Nakatsuji, M. Hada, M. Ehara, K. Toyota, R. Fukuda, J. Hasegawa, M. Ishida, T. Nakajima, Y. Honda, O. Kitao, H. Nakai, M. Klene, X. Li, J. E. Knox, H. P. Hratchian, J. B. Cross, V. Bakken, C. Adamo, J. Jaramillo, R. Gomperts, R. E. Stratmann, O. Yazyev, A. J. Austin, R. Cammi, C. Pomelli, J. W. Ochterski, P. Y. Ayala, K. Morokuma, G. A. Voth, P. Salvador, J. J. Dannenberg, V. G. Zakrzewski, S. Dapprich, A. D. Daniels, M. C. Strain, O. Farkas, D. K. Malick, A. D. Rabuck, K. Raghavachari,J. B. Foresman, J. V. Ortiz, Q. Cui, A. G. Baboul, S. Clifford, J. Cioslowski, B. B. Stefanov, G. Liu, A. Liashenko, P. Piskorz, I. Komaromi, R. L. Martin, D. J. Fox, T. Keith, M. A. Al-Laham, C. Y. Peng, A. Nanayakkara, M. Challacombe, P. M. W. Gill, B. Johnson, W. Chen, M. W. Wong, C. Gonzalez, J. A. Pople, Gaussian, Inc., Wallingford CT, USA, **2004**.
[36] a) J. P. Perdew, K. Burke, M. Ernzerhof, *Phys. Rev. Lett.* **1996**, *77*, 3865; b) W. Kutzelnigg, U. Fleischer, M. Schindler, *NMR-Basic Principles and Progress, Vol. 23.* Springer, Heidelberg, **1990**, p. 165.
[37] A. M. Köster, P. Calaminici, R. Flores-Moreno, G. Geudtner. A. Goursot, T. Heine, F. Janetzko, J. U. Reveles, A. Vela, S. Patchkovskii, D. R. Salahub, *deMon2k*; NRC: Ottawa, Canada, **2003**; http://www.de-Mon-software.com.
[38] W. Kutzelnigg, *Isr. J. Chem.* **1980**, *19*, 193.
[39] J. Pipek, P. G. Mezey, *J. Chem. Phys.* **1989**, *90*, 4916.
[40] V. G. Malkin, O. L. Malkina, D. R. Salahub, *Chem. Phys. Lett.* **1993**, *204*, 80.
[41] a) F. Schönborn, H. Schmitt, H. Zimmermann, U. Haeberlen, C. Corminboeuf, G. Großmann, T. Heine, *J. Magn. Reson.* **2005**, *175*, 52; b) T. Heine, C. Corminboeuf, G. Grossmann, U. Haeberlen, *Angew. Chem.* **2006**, *118*, 7450; *Angew. Chem. Int. Ed.* **2006**, *45*, 7292.

Received: March 8, 2012
Published Online: ■

Zeitschrift für anorganische und allgemeine Chemie ZAAC Journal of Inorganic and General Chemistry